Halvor Dalaker* and Merete Tangstad

The Interactions of Carbon and Nitrogen in Liquid Silicon

Abstract: The interactions between carbon and nitrogen in liquid silicon have been studied experimentally. High purity silicon was melted in silicon nitride crucibles under an Ar atmosphere with a graphite slab inserted in the crucible prior to melting as a carbon source. The system was thus simultaneously equilibrated with Si_3N_4 and SiC. Samples were extracted in the temperature range 1695–1798 K and analyzed using Leco.

It was observed that the simultaneous saturation of nitrogen and carbon caused a significant increase in the solubilities of both elements. The interaction parameters were derived as

$$e_C^N = 95.01 \pm 1 - \frac{177555 \pm 10000}{T}$$

$$e_N^C = 110.83 \pm 1.2 - \frac{207123 \pm 12000}{T}$$

The solubility of carbon in liquid silicon as a function of temperature and nitrogen content was found to follow:

$$C_C(T, C_N) = (7.37 \pm 0.11)\ \exp\left[-\frac{(11731 \pm 197)}{T} - \left(95.01 \pm 1 - \frac{177555 \pm 10000}{T} \right) C_N \cdot \ln(10) \right]$$

And the solubility of nitrogen in liquid silicon found to follow:

$$C_N(T, C_C) = 7957.9 \cdot \exp\left[-\frac{24376}{T} - \left(110.83 \pm 1.2 - \frac{207123 \pm 12000}{T} \right) C_C \cdot \ln(10) \right]$$

Keywords: silicon, termodynamics, interaction coefficients

PACS® (2010). 81.05.Bx

***Corresponding author: Halvor Dalaker:** SINTEF Materials and Chemistry, Trondheim, Norway. E-mail: halvor.dalaker@sintef.no
Merete Tangstad: Norwegian University of Science and Technology, Trondheim, Norway

1 Introduction

The casting of multi crystalline silicon ingots for solar applications typically takes place in fused silica crucibles that are coated with silicon nitride to avoid sticking. When the silicon melts, this coating will dissolve and nitrogen will be incorporated into the silicon melt.

Furthermore, both the susceptor and a large portion of the insulation of the induction furnaces used are made from graphite. This carbon rich environment enriches the silicon melt through interactions in the gas phase.

Upon solidification, this nitrogen and carbon may re-precipitate as carbide and nitride particles, which have been associated with negative impacts on solar cell operation. Binetti et al. [1] associated a drop in minority carrier lifetime with high levels of silicon nitrides. The carbide particles can act as nucleation sites for dislocations [2] which are detrimental to solar cell operation [3]. Silicon nitride can also cause an increased dislocation density: either directly by acting as nucleation sites for dislocations, or indirectly by nucleating SiC particles which in turn create dislocations [2]. Such dislocations have been estimated to lower the efficiency of the finished solar cell with as much as 3–4 percentage points [3].

Furthermore, nitride particles have been observed as the starting point for the growth of silicon carbide filaments. These filaments typically grow in the direction of solidification and can therefore easily intercept the pn-junction of a finished cell and cause shunting [4].

In understanding the formation of silicon nitride and carbide particles and their interactions with one another, the solubility limits of carbon and nitrogen in liquid silicon are important figures.

The present authors have previously published the solubilities of both carbon and nitrogen in liquid silicon in the pure Si–C and Si–N systems [5, 6]. In the current work, the same experimental set up is used to investigate the interactions between carbon and nitrogen in liquid silicon and specifically how these interactions affect the solubility limits during simultaneous saturation.

In the current work, liquid silicon melts have been equilibrated with silicon nitride and silicon carbide under an Ar atmosphere, and samples have been extracted and analyzed for carbon and nitrogen content.

The new results have been discussed together with those previously reported on the pure Si–C and Si–N systems to derive the C–N-interaction coefficient.

2 Experimental

In each experiment, approximately 75 g of high purity polycrystalline silicon feedstock was charged in a crucible. For the experiments in the Si–C–N-system, a reaction bonded silicon nitride (Morgan Ceramics) crucible was used, and prior to charging a slab of high density graphite (Tanso IG-610) was inserted in the crucible to act as a carbon source. In the experiments in the pure Si–N system a silicon nitride crucible with no graphite slab was used, and for the pure Si–C system a graphite crucible (Tanso IG-610) was used.

The starting concentrations of nitrogen and carbon were investigated through analysis of six silicon feedstock samples. The average carbon concentration was found to be $9 \cdot 10^{-4}$ mass% with a standard deviation of $3 \cdot 10^{-4}$ mass%. In the case of nitrogen three samples had a nitrogen level below the detection limit of $2 \cdot 10^{-4}$ mass% while the remaining three had nitrogen levels of $2 \cdot 10^{-4}$ mass%.

The silicon was then melted in a resistance heated tube furnace. Once the silicon had melted liquid silicon reacted with the graphite to form SiC. Carbon and nitrogen could then enter the melt through the following equilibrium reactions:

$$SiC_{(s)} \rightleftharpoons Si + \underline{C} \quad (1)$$

$$Si_3N_{4(s)} \rightleftharpoons 3Si_{(liq)} + 4\underline{N} \quad (2)$$

where $\underline{C}$ ($\underline{N}$) means carbon (nitrogen) dissolved in liquid silicon with the standard state of 1 mass% carbon (nitrogen).

Nitrogen and carbon would continue to enter the melt until the liquid was saturated locally. The melt flow would then transport the solutes away from the Si_3N_4/SiC, allowing more solute to enter into solution. This process would continue until the solute content of the melt was uniform and equal to the saturation limits. As already discussed elsewhere [5, 6], the saturation limit is reached quickly in this set-up – within a few minutes at most – and the gas-phase transport of nitrogen as N_2 needs not be considered as it has been shown to be insignificant [6].

A sketch of the furnace is seen in Figure 1. The top flange of the furnace has three inlets, one of which was used for flow of Ar-gas into the furnace. Of the remaining

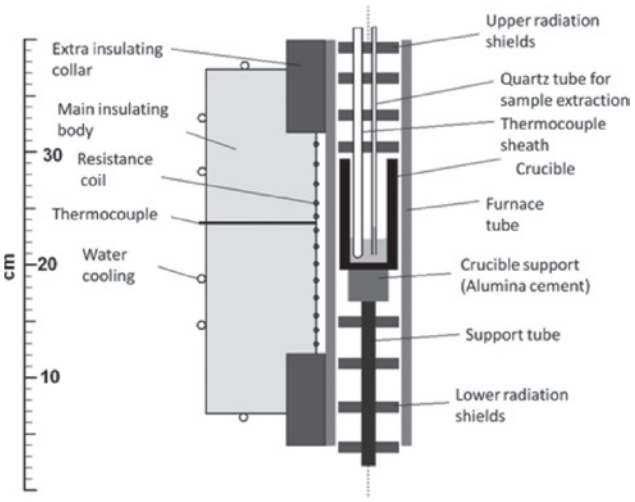

Fig. 1: Sketch of the interior of the tube furnace. The insulation and water cooling have been excluded on the right hand side of the figure.

two inlets, one was used for an alumina sheath, inside which was nested a type S Pt-Pt10%Rh thermocouple measuring the melt temperature. Another thermocouple was placed near the hottest point on the heating spiral, and used to control the furnace temperature with a Eurotherm 903P temperature controller. All temperature measurements in this article refer to the melt temperature.

The final inlet was used for the sample taking and is fitted with a ball valve, a 115 mm long steel tube, and a sealing mechanism with two o-rings. The samples were extracted using quartz tubes fitted with a syringe.

In each sampling, ~0.5 mL (~1 g) melt was sucked into the tube, meaning that roughly 130–140 mm of the tube was filled with silicon. Since the distance between the ball valve and the bottom o-ring was 160 mm, this prevented damage to the o-ring seal, as the valve could be closed beneath the nozzle of the sampling tube with all the hot silicon inside the metal tube still below the o-ring.

As samples were extracted at different temperatures during one experimental run, the samples were always taken in order of increasing temperature to avoid the formation of precipitates. Such precipitates would give too high carbon and nitrogen levels during analysis.

The samples were etched in concentrated HF for a couple of days in order to completely get rid of the quartz tubes. The silicon was then rinsed in distilled water and sent to analysis at Elkem Research where they were analyzed using Leco. For nitrogen a Leco TCH600 analyzer was used, while a Leco C200 was used to determine the carbon levels. It was confirmed through microprobe analysis that no SiC or Si_3N_4 precipitated on the inside of the

quartz tubes, hence no nitrogen or carbon was lost during the etching process.

3 Results and discussion

Six experimental runs were conducted in the Si–C–N-system from which 33 samples were extracted in the temperature range 1695–1798 K. Each sample was divided and analyzed in two to three parallels each. Because of limitations in the sample size, each sample could not be analyzed for both carbon and nitrogen. Therefore, half the samples were analyzed for carbon, while the other half was analyzed for nitrogen.

In the pure Si–C-system, four experimental runs between 1687 and 1832 K yielded 39 samples, and in the pure Si–N-system, four experimental runs gave 61 samples in the range 1701–1815 K. These samples were analyzed for C and N respectively.

As was already reported elsewhere [5, 6], the carbon and nitrogen solubilities in the pure Si–C and Si–N systems were found to follow:

$$C_C(T) = 839.4 \cdot \exp(-19856/T) \quad (3)$$

$$C_N(T) = 7957.9 \cdot \exp(-24376/T) \quad (4)$$

where C_X is the concentration, in mass%, of element X in liquid silicon at temperature T. These results generally agreed well with other data from literature [5, 6].

The experimental data from the Si–C–N-system were used in the fitting of two exponential expressions describing the carbon and nitrogen levels as functions of absolute temperature:

$$C_C^{N_{sat}}(T) = 38.8 \pm 0.2 \cdot \exp\left[-\frac{14420 \pm 284}{T}\right] \quad (5)$$

$$C_N^{C_{sat}}(T) = (5.84 \pm 0.06) \cdot 10^3 \cdot \exp\left[-\frac{23451 \pm 108}{T}\right] \quad (6)$$

Here, $C_X^{Y_{sat}}$ signifies the concentration, in mass%, of element X under simultaneous saturation with element Y. The fitting of these expressions do not take the presence of element Y into account, but only looks at the relationship between the concentration of X and the temperature T. Since the C–C and N–N interactions were found to be insignificant in previous work and in literature [5–8], the e_C^C and e_N^N are also left out. In other words, the expressions (5) and (6) are fitted under the (unrealistic) assumption that the conditions are the same as in the pure Si–C and Si–N-systems. Thus, if the presence of an element Y had no influence on the solubility of element X, one would expect Eqs. 5 and 6 to correlate closely to Eqs. 3 and 4 respectively.

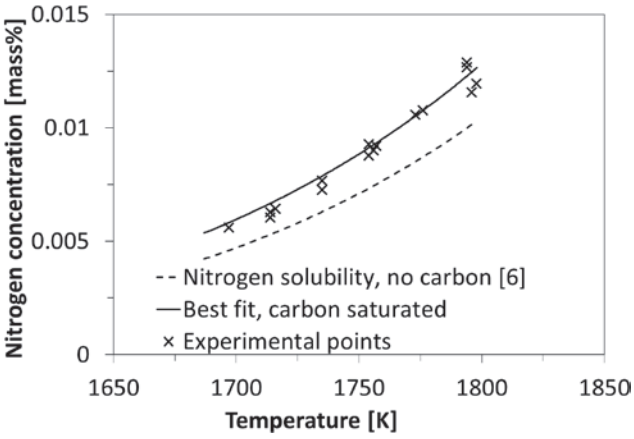

Fig. 2: The best fit equations for the solubility of nitrogen in liquid silicon. The dashed curve indicates the solubility limit in the pure Si–N-system [6], while the solid curve and the experimenntal points indicate the solubility in the carbon-saturated Si–C–N-system.

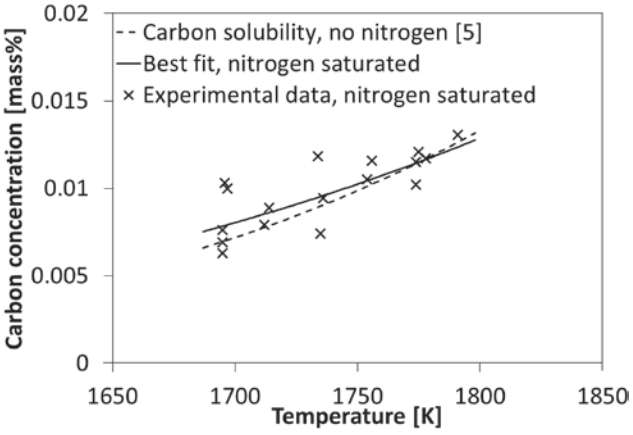

Fig. 3: The best fit equations for the solubility of carbon in liquid silicon. The dashed curve indicates the solubility limit in the pure Si–C-system [5], while the solid curve and experimental points indicates the solubility in the nitrogen-saturated Si–C–N-system.

Eqs. 3–6 are displayed in Figures 2 and 3 together with the experimental points from the current work.

It can be seen that the predicted nitrogen solubility is higher at all temperatures for the carbon-saturated case; i.e. Eq. 4 does not correspond well with Eq. 6, meaning that the presence of carbon influences the nitrogen solubility.

The case for carbon-solubility is not so straightforward, as the two solubility curves can be seen to intersect at approximately 1775 K.

This is caused by two data points at 1833 K in the pure Si–C-system predicting a very high solubility [5]. This data

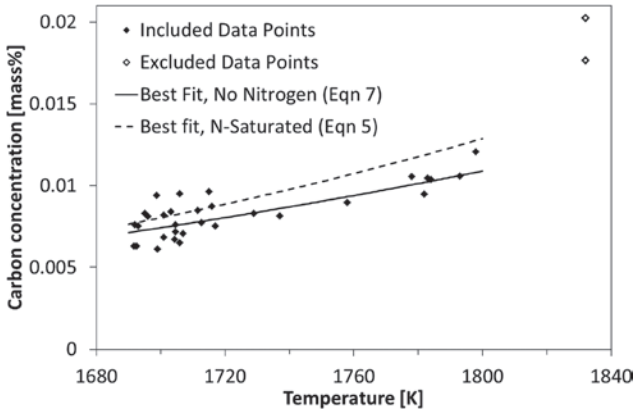

Fig. 4: The re-evaluated best fit equation for the solubility of carbon in liquid silicon for the pure Si–C-system, together with the included and excluded data points [5].

point lies well outside the temperature range of the experiments performed during nitrogen-saturation, and the inclusion of this data point in the comparison of the two data sets is thus debatable. For this reason, a new exponential expression was fitted to the data obtained from the pure Si–C system in the temperature range between 1687 K–1793 K. The resulting equation was:

$$C_C(T) = (7.37 \pm 0.11) \cdot \exp(-11731 \pm 197/T) \tag{7}$$

This equation is plotted in Figure 4 together with the original data points from the pure Si–C-system and the curve describing Eq. 5. From this figure it is seen that the solubility curve for the pure Si–C-system lies well below the curve for the nitrogen-saturated system, which is analogous to the case for nitrogen solubility under carbon saturation.

Even when including values only below 1793 K, the scatter in the experimental data points detracts from the clear impression that the carbon solubility increases in the presence of nitrogen. This is mainly caused by the inhomogeneous distribution of carbon in the samples. However, as the interaction coefficients are tied together by the relation

$$\varepsilon_B^A = \frac{\partial^2 \Delta G/RT}{\partial N_B \partial N_A} = \frac{\partial^2 \Delta G/RT}{\partial N_A \partial N_B} = \varepsilon_A^B \tag{8}$$

the clear picture for the case of nitrogen solubility confirms the trend observed for carbon solubility. It is therefore evident that the solubilities of both carbon and nitrogen increase during simultaneous saturation, meaning that the interaction coefficients e_N^C and e_C^N are both negative.

Since the Si(l), SiC(s) and Si_3N_4(s) phases are all virtually pure, the equilibrium constants of Eqs. 1 and 2 can be approximated as:

$$K_1 = \frac{1}{a_C}, \quad K_2 = \frac{1}{a_N^4} \tag{9,10}$$

With 1 mass% solutions as the standard states, one can write

$$\log(K_1) = -\log(f_C) - \log(C_C) \tag{11}$$

$$(1/4) \cdot \log(K_2) = -\log(f_N) - \log(C_N) \tag{12}$$

where f_C and f_N are the activity coefficients of carbon and nitrogen with Henrian standard sates. In terms of interaction parameters:

$$\log(f_C) = e_C^C \cdot C_C + e_C^N \cdot C_N \tag{13}$$

$$\log(f_N) = e_N^N \cdot C_N + e_N^C \cdot C_C \tag{14}$$

where higher order terms have been ignored, and it is assumed that no other impurities are present to influence f_C and f_N. Since the solubilities in the pure Si–C and Si–N systems were found to follow Henry's Law behavior [5, 6], it follows that the self interaction coefficients e_C^C and e_N^N are negligible. The temperature dependence of the interaction parameters follows $e = \alpha + \beta/T$; and since $M_N \approx M_C$, the approximation $e_N^C = M_N/M_C \cdot e_C^N$ can be made and the following expressions can be derived for the solubilities:

$$C_C(T, C_N) = \frac{1}{K_1(T)} \cdot \exp\left[-\left(\alpha + \frac{\beta}{T}\right) C_N \cdot \ln(10)\right] \tag{15}$$

$$C_N(T, C_C) = \frac{1}{K_2(T)^{1/4}} \cdot \exp\left[-\left(\frac{M_N}{M_C}\right) \cdot \left(\alpha + \frac{\beta}{T}\right) C_C \cdot \ln(10)\right] \tag{16}$$

These equations must approach the solubilities in the pure Si–C and Si–N systems when the amount of the second solute approaches zero, which means that the pre-exponential factors can be replaced by the expressions for the pure Si–C and Si–N-systems (Eqn. 4, 7):

$$C_C(T, C_N) = 7.37 \pm 0.11 \cdot \exp\left[-\frac{(11731 \pm 197)}{T} - \left(\alpha + \frac{\beta}{T}\right) C_N \cdot \ln(10)\right] \tag{17}$$

$$C_N(T, C_C) = 7957.9 \cdot \exp\left[-24376/T - \left(\frac{M_N}{M_C}\right) \cdot \left(\alpha + \frac{\beta}{T}\right) C_C \cdot \ln(10)\right] \tag{18}$$

α and β were determined by fitting the experimental data using the method of least squares. Since the extracted samples were analyzed for carbon or nitrogen only, in the fitting of the data the concentration of the element that was not measured for each sample was calculated using the found Eqs. 3 and 4. The best fit of the experimental data resulted in:

$$e_C^N = 95.01 \pm 1 - \frac{177555 \pm 10000}{T} \tag{19}$$

$$e_N^C = 110.83 \pm 1.2 - \frac{207123 \pm 12000}{T} \tag{20}$$

The accuracies of alpha and beta has not been rigorously determined, but based on the accuracies of the parameters in the solubility expressions, the worst case is an error in the second significant digit. These equations are valid between 1695 and 1798 K. Using these expressions in Eqs. 17 and 18, one obtains expressions showing the solubility of carbon as a function of temperature and nitrogen content, as well as the nitrogen solubility as a function of temperature and carbon content in the temperature range between 1695 and 1798 K:

$$C_C(T, C_N) = (7.37 \pm 0.11)\ \exp\left[-\frac{(11731 \pm 197)}{T} - \left(95.01 \pm 1 - \frac{177555 \pm 10000}{T} \right) C_N \cdot \ln(10) \right] \tag{21}$$

$$C_N(T, C_C) = 7957.9 \cdot \exp\left[-24376/T - \left(110.83 \pm 1.2 - \frac{207123 \pm 12000}{T} \right) C_C \cdot \ln(10) \right] \tag{22}$$

Assuming only first-order interactions, these equations will be valid up to the saturation limit of the secondary impurity. They are therefore useful for calculating the solubility limit of carbon or nitrogen in situations where the other element is present in small and known quantities. One example could be the estimation of the carbon content in a silicon melt held in a graphite crucible in a nitrogen free environment when the silicon feedstock contains a known amount of nitrogen.

In the situation where the melt is simultaneously saturated with both carbon and nitrogen, such as is the case in the experimental set-up of the current work, the equations cannot be used so straightforwardly, since the carbon saturation limit depends on the nitrogen saturation limit and vice versa. At a given temperature, one basically has to find the solutions to a set of equations in the form of:

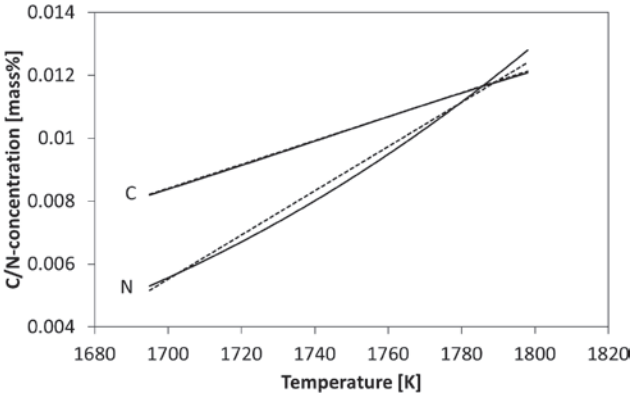

Fig. 5: Solubility limits of carbon and nitrogen as functions of temperature during simultaneous saturation. The solid curves represent the iterative solutions of Eqs. 19 and 20, while the dashed lines are the linear approximations of Eqs. 25 and 26.

$$C_C = a \cdot \exp(b \cdot C_N) \tag{23}$$

$$C_N = c \cdot \exp(d \cdot C_C) \tag{24}$$

which cannot be done analytically. Thus, a numerical or iterative solution method must be employed. An iterative solution method was chosen in the present work, and the resulting solubility limits are plotted in Figure 5. It can be seen that the solubility limits depend almost linearly on temperature. Therefore, linear approximations were constructed for the solubility of carbon and nitrogen as functions of temperature during simultaneous saturation:

$$C_C^{N_{sat}} = 3.80 \cdot 10^{-5} T - 5.62 \cdot 10^{-2} \tag{25}$$

$$C_N^{C_{sat}} = 7.03 \cdot 10^{-5} T - 0.114 \tag{26}$$

These approximations are valid in the temperature regime of the current work, i.e. between 1695–1798 K. The R^2 between the linear and non-linear model was greater than 0.99 in both regressions.

4 Conclusions

The interactions between carbon and nitrogen in liquid silicon have been studied experimentally. It was observed that the simultaneous saturation of these elements caused a significant increase in the solubilities of both elements. The interaction parameters were derived as

$$e_C^N = 95.01 \pm 1 - \frac{177555 \pm 10000}{T}$$

$$e_N^C = 110.83 \pm 1.2 - \frac{207123 \pm 12000}{T}$$

The solubility of carbon in liquid silicon as a function of temperature and nitrogen content was found to follow:

$$C_C(T,C_N) = (7.37 \pm 0.11)\ \exp\left[-\frac{(11731 \pm 197)}{T} - \left(95.01 \pm 1 - \frac{177555 \pm 10000}{T} \right) C_N \cdot \ln(10) \right]$$

and the solubility of nitrogen in liquid silicon found to follow:

$$C_N(T,C_C) = 7957.9 \cdot \exp\left[-24376/T - \left(110.83 \pm 1.2 - \frac{207123 \pm 12000}{T} \right) C_C \cdot \ln(10) \right]$$

Linear approximations to the solubility levels during simultaneous saturation were derived as

$$C_C^{N_{sat}} = 3.80 \cdot 10^{-5} T - 5.62 \cdot 10^{-2}$$
$$C_N^{C_{sat}} = 7.03 \cdot 10^{-5} T - 0.114$$

Acknowledgments: The authors wish to thank The Norwegian Research Council, The Norwegian Ferroalloy Producers Research Assosiation (FFF) and all other financial contributors to the ThermoTech project through which the current work has been performed. Heartfelt thanks are also due Elkem for the performance of chemical analysis without charge.

Received: May 6, 2013. Accepted: October 12, 2013.

References

[1] S. Binetti, M. Acciarri, C. Savigni, A. Brianza, S. Pizzini and A. Musinu, *Mater. Sci. Eng. B*, 36 (1996) 68–72.
[2] B. Ryningen, K. S. Sultana, E. Stubhaug, O. Lohne and P. C. Hjelmås, Proc. 22nd EU-PV Solar Energy Conf., 2007, pp. 1086–1090.
[3] B. Sopori, C. Li, S. Narayanan and D. Carlson, Mater. Res. Soc. Symp. Proc., 2005, p. 864.
[4] J. Bauer, O. Breitenstein and J.-P. Rakotoniaina, *Phys. Status Solidi A*, 204 (2007) 2190–2195.
[5] H. Dalaker and M. Tangstad, *Mater. Trans.*, 50 (2009) 1152–1156.
[6] H. Dalaker and M. Tangstad, *Mater. Trans.*, 50 (2009) 2541–2544.
[7] K. Yanaba, M. Akasaka, M. Takeuchi, M. Watanabe, T. Narushima and Y. Iguchi, *Mater. Trans. JIM*, 38 (1997) 990–994.
[8] T. Narushima, N. Ueda, M. Takeuchi, F. Ishii and Y. Iguchi, *Mater. Trans. JIM*, 35 (1994) 821–826.